Manifestation of quadrupole hyperfine interaction and of interlevel interaction in the optical spectrum of the $LiYF_4$:Ho crystal

N. I. Agladze, E. A. Vinogradov, and M. N. Popova

Spectroscopy Institute, USSR Academy of Sciences
(Submitted 12 December 1985)
Zh. Eksp. Teor. Fiz. **91**, 1210–1218 (October 1986)

The nonequidistance of the hyperfine structure of the lines in the absorption spectra of the $LiYF_4$:Ho is investigated in the region of the $^5I_8$-$^5I_{7,6}$ transitions in the Ho^{3+} ion. The experimental data are compared with perturbation-theory calculations of the electric quadrupole interaction with the nucleus and of the magnetic hyperfine interaction in second order. The electric-field gradients at the holmium nucleus are estimated.

$LiYF_4$ crystals activated with rare earths are attracting attention both as promising laser materials[1] and as relatively simple and convenient model systems for the study of the crystal field,[2] of electron-phonon[5] and spin-spin[6] interactions, and of magnetic phase transitions.[7,8]

The first observation of nuclear hyperfine structure in the optical crystal of the $LiYF_4$:Ho crystal and an investigation of the magnetodipole electron-nucleus interaction were reported in Ref. 9. The present paper is devoted to the results of a study of the nonequidistance in the hyperfine structure of the lines. We show that the nonequidistance can be well explained qualitatively by taking into account the electric quadrupole interaction in first-order perturbation theory and of the magnetic dipole interaction in second order. The experimental data are quantitatively compared with a calculation in which the wave functions of the crystal-field levels are used.

We have investigated the polarized absorption spectra of an $LiYF_4$:Ho (about 1% wt.%) crystal grown by the Czochralski method in the region of the $^5I_8 \rightarrow {}^5I_{7,6}$ transitions in the Ho^{3+} ion, with spectral resolution down to 0.01 cm^{-1}, using the special UFS-02 high-resolution Fourier spectrometer.[10] The crystal was kept in a cryostat in helium vapor at a temperature 6.2 K stabilized to within ± 0.1 K.

The spectra reveal a well-resolved structure due to the hyperfine interactions of the electrons and the nuclei of the only isotope ^{165}Ho having an angular momentum $I = 7/2$ (see Fig. 1). The individual hyperfine components are 0.03–0.05 cm^{-1} wide in the low-frequency part of each of the $^5I_8 \rightarrow {}^5I_{7,6}$ transitions, whereas the high-frequency lines are strongly broadened by nonradiative transitions to lower components of the Stark multiplet with creation of lattice phonons.[9]

The hyperfine structure (hfs) of the levels is due to the coupling of the electrons with the electric and magnetic moments of the nucleus, and is described by the Hamiltonian[11]

$$\mathcal{V} = A_J \mathbf{JI} + \frac{B_J}{2I(2I-1)J(2J-1)} \times \left\{ 3(\mathbf{JI})^2 + \frac{3}{2}\mathbf{JI} - I(I+1)J(J+1) \right\}, \quad (1)$$

where

$$A_J = 2\beta\beta_I g_I \langle r^{-3} \rangle \langle J \| N \| J \rangle + A_s', \quad (2a)$$

$$A_s' = -2.8 \cdot 10^{-3} g_I (\langle J \| \Lambda \| J \rangle - 1) \text{ см}^{-1}, \quad (2b)$$

$$B_J = -J(2J-1) e^2 Q \langle r^{-3} \rangle (1 - R_q) \langle J \| \alpha \| J \rangle. \quad (3)$$

The first term of the Hamiltonian represents the interaction between the magnetic-dipole moment of the nucleus and the magnetic field produced at the nucleus by the electrons. The second term describes the interaction between the electric quadrupole moment of the nucleus and the electric-field gradient at the nucleus. In Eqs. (2) and (3), β is the Bohr magneton, β_I the nuclear magneton, g_I the nuclear g factor, Q the quadrupole moment of the nucleus, and $\langle r^{-3} \rangle$ the average reciprocal cube of the radius of the electron orbitals. The Sternheimer antiscreening factor R_q takes into account the contribution made to the electric-field gradient at the nucleus by the polarization of the electron shells by the electrons of the unfilled f shell. $\langle J \| N \| J \rangle$, $\langle J \| \Lambda \| J \rangle$, $\langle J \| \alpha \| J \rangle$ are the reduced matrix elements defined, e.g., in Ref. 11. The quantity $\text{Å}_s'$ in the constant A_J of the magnetic hfs takes into account the core polarization and the relativistic contribution.[11]

The interaction (1) is small compared with the interaction between the impurity-ion electrons and the electric field (which is in turn smaller in rare-earth ions than the interactions that form the free-ion spectrum), and its influence on the ion levels in the crystal field can be taken into account by perturbation theory. For the electric quadrupole interaction, which is substantially weaker than the magnetic dipole interaction, first-order perturbation theory is sufficient.

The impurity rare-earth ion replaces yttrium in the $LiYF_4$ lattice that has the scheelite structure (space group C_{4h}^6) and occupies a tetragonal position with point group S_4. For an ion with an even number of electrons, such as Ho^{3+}, the crystal field of symmetry S_4 has nondegenerate levels Γ_1 and Γ_2 and doubly degenerate Γ_{34} (the irreducible representations of Γ_3 and Γ_4 are Kramers-conjugate). The correction to the energy E_m of the state $|\Gamma_m\rangle|M\rangle$ ($m = 1,2,3,4$; $-I \leqslant M \leqslant I$, M is the axial component of the nuclear moment) is given by

$$\Delta E(\Gamma_m M) = A_J \langle \Gamma_m | J_z | \Gamma_m \rangle + \frac{3B_J \langle \Gamma_m | 3J_z^2 - J(J+1) | \Gamma_m \rangle}{4I(2I-1)J(2J-1)}$$

 0038-5646/86/100716-05$04.00

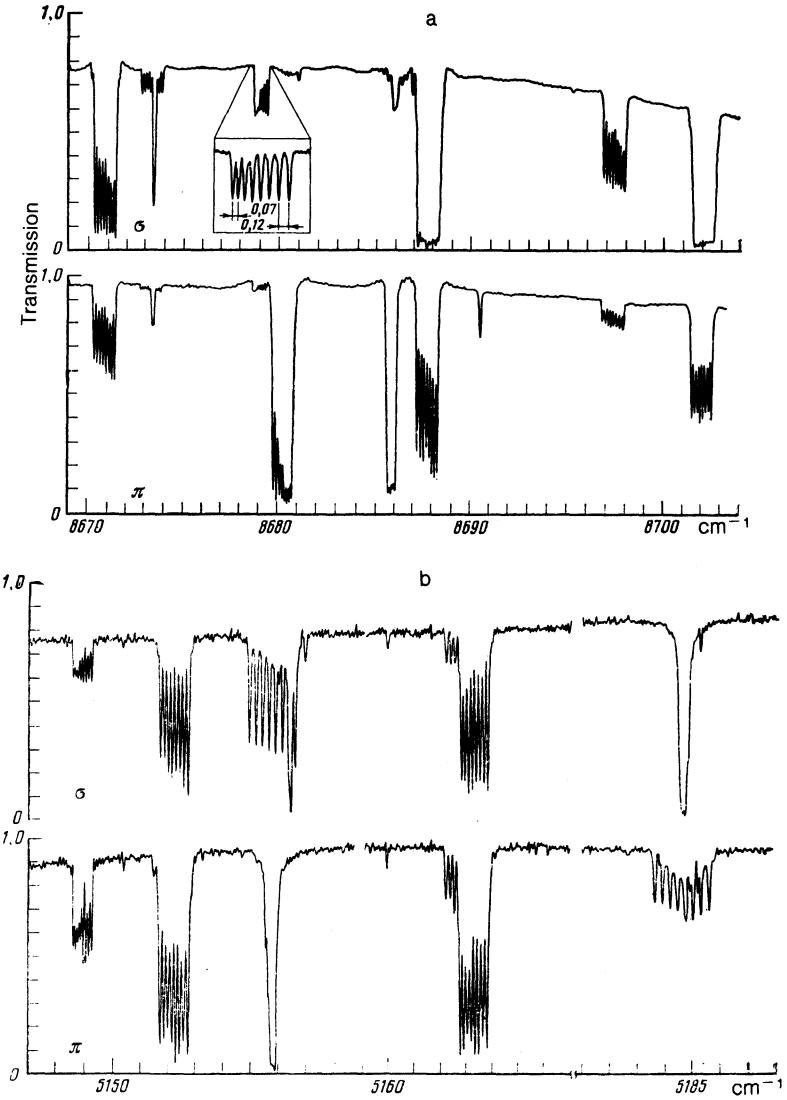

FIG. 1. Absorption of $LiYF_4:Ho^{3+}$ crystal at 6.2 K in the region of the transitions ${}^5I_8 \rightarrow {}^5I_6$ (a) and ${}^5I_8 \rightarrow {}^5I_7$ (b) for $\mathbf{E} \| c$ (π) and $\mathbf{E} \perp c$ (σ) polarizations. Spectral resolution interval 0.04 cm^{-1}. The line with pronounced nonequidistance in the center is from a spectrum with 0.01 cm^{-1} resolution.

$$\times\left[M^2-\frac{I(I+1)}{3}\right]+\sum_i \frac{A_J^2|\langle\Gamma_m^{(i)}|J_z|\Gamma_m\rangle|^2}{E(\Gamma_m M)-E(\Gamma_m^{(i)}M)}M^2$$

$$+\sum_{i,n\neq m}\frac{1}{4}\left\{\frac{A_J^2|\langle\Gamma_n^{(i)}|J_+|\Gamma_m\rangle|^2}{E(\Gamma_m M)-E(\Gamma_n^{(i)}M-1)}[I(I+1)-M(M-1)]\right.$$

$$\left.+\frac{A_J^2|\langle\Gamma_n^{(i)}|J_-|\Gamma_m\rangle|^2}{E(\Gamma_m M)-E(\Gamma_n^{(i)}M-1)}[I(I+1)-M(M+1)]\right\}, \quad (4)$$

where

$$E(\Gamma_m M)=E_m+A_J\langle\Gamma_m|J_z|\Gamma_m\rangle M, \quad (5)$$

the index i numbers the representations Γ_m, while the operators J_+ and J_- are defined as usual, viz., $J_+ = J_x + iJ_y$, $J_- = J_x - iJ_y$. The matrix elements in (4) satisfy the following relations that follow from the symmetry properties, including time reversal:

$$\langle\Gamma_m|J_z|\Gamma_m\rangle=0, \quad m=1,2; \quad \langle\Gamma_1|J_z|\Gamma_4\rangle=-\langle\Gamma_3|J_z|\Gamma_3\rangle, \quad (6)$$

$$\langle\Gamma_4|3J_z^2-J(J+1)|\Gamma_4\rangle=\langle\Gamma_3|3J_z^2-J(J+1)|\Gamma_3\rangle, \quad (7)$$

$$\langle\Gamma_2|J_+|\Gamma_3\rangle=-\langle\Gamma_2|J_-|\Gamma_4\rangle^*=2\langle\Gamma_2|J_x|\Gamma_3\rangle, \quad (8a)$$

$$\langle\Gamma_2|J_-|\Gamma_3\rangle=\langle\Gamma_2|J_+|\Gamma_4\rangle=\langle\Gamma_2|J_\pm|\Gamma_1\rangle=\langle\Gamma_2|J_z|\Gamma_1\rangle=0. \quad (8b)$$

It can be seen from (4)–(8) that the hyperfine sublevels of the level Γ_m are doubly degenerate in the projections of the angular momentum: the state pairs

$|\Gamma_m\rangle|M\rangle$ и $|\Gamma_m\rangle|-M\rangle$, $m=1$ or 2;

$|\Gamma_3\rangle M\rangle$and$|\Gamma_4\rangle|-M\rangle$

have equal energies.

The first term of (4) describes an equidistant magnetic hfs of first order and makes the largest contribution to the structure of the degenerate electronic level Γ_{34}. There is no magnetic hfs in first order for nondegenerate levels [see (6)]. The magnetic hyperfine structure can be treated as the Zeeman splitting of a degenerate electron Stark level in the nuclear magnetic field that is quantized in accordance with

the quantization of the projection of the nuclear moment on the symmetry axis.

The second term in (4) comprises the shift and the nonequidistant hfs due to the electric quadrupole interaction, a structure allowed for all the Γ_m representations.

The first sum in (4) gives the mutual repulsion of the hyperfine components of the interacting levels Γ_{34} and describes the magnetic hfs of the interacting nondegenerate electronic levels Γ_1 or Γ_2 due to the off-diagonal matrix elements $A_J J_z I_z$ of the magnetic hyperfine interaction. The operator $A_J(J_z I_x + J_y I_y)$ has only off-diagonal matrix elements in the group S_4, and furthermore between states of unlike symmetry. Its contribution is the second sum of (4).

Transforming this sum with allowance for (5) and (8) we obtain for the corrections δ_n ($n = 1,2$) and δ_3 to the energies of the levels Γ_n ($n = 1,2$) and Γ_{34}, due to the interaction with levels of different symmetry, the following expressions:

$$\delta_n = 2[I(I+1)-M^2] \times \sum_i \frac{A_J^2 |\langle \Gamma_3^{(i)} | J_x | \Gamma_n \rangle|^2}{(E_n - E_{34}^{(i)})\{1-[A^{(i)}M/(E_n-E_{34}^{(i)})]^2\}}, \quad (9)$$

$$\delta_3 = [I(I+1)-M^2+M] \times \sum_{i;n=1,2} \frac{A_J^2 |\langle \Gamma_n^{(i)} | J_x | \Gamma_3 \rangle|^2}{(E_{34}-E_n^{(i)})\{1+[AM/(E_{34}-E_n^{(i)})]\}}, \quad (10)$$

where

$$A = A_J \langle \Gamma_3 | J_z | \Gamma_3 \rangle, \quad A^{(i)} = A_J \langle \Gamma_3^{(i)} | J_z | \Gamma_3^{(i)} \rangle.$$

As a result we can write for the total energy of the hyperfine sublevel

$$E_{n,M} = E_n + (2D - B/3) I(I+1) + (B+C-2D)M^2, \quad n=1,2; \quad (11)$$

$$E_{3,M} = E_{4,-M} = E_{34} + (D-B/3) I(I+1) + (A+D)M + (B+C-D)M^2. \quad (12)$$

Here B is the coefficient of M^2 in the quadrupole term of (4), C is the sum preceeding M^2 in the correction to the energy for the interaction of levels of like symmetry in (4), and D is the sum in (9) or (10) for the correction to the energy for the interaction of levels of unlike symmetry. The coefficients C and D depend, generally speaking, on m. This dependence can be neglected when the distance between the levels is much larger than the hyperfine splitting. It can be seen that the electric quadrupole interaction and the off-diagonal matrix element of the magnetic dipole interaction produce in the hfs a nonequidistance of like type. The interaction between levels of like symmetry leads here to a mutual repulsion of their hyperfine components, whereas the components of levels having unlike symmetry seem to be mutually attracted. By way of example, Fig. 2 shows the hfs of different interacting levels.

The frequencies in a spectral line are determined by the difference between energies, similar to (11) and (12), of the final and initial states with allowance for the selection rules. The allowed transitions are the electrodipole $\Gamma_1 \leftrightarrow \Gamma_2$, $\Gamma_3 \leftrightarrow \Gamma_4$ in π polarization and Γ_1, $\Gamma_2 \leftrightarrow \Gamma_3$, Γ_4 in σ, and the magnetodipole Γ_1, $\Gamma_2 \leftrightarrow \Gamma_3$, Γ_4 in π polarization and $\Gamma_1 \to \Gamma_1$, $\Gamma_2 \to \Gamma_2$, $\Gamma_3 \to \Gamma_3$, $\Gamma_4 \to \Gamma_4$ in σ. In this case $\Delta M = 0$. As a result, the lines Γ_1, $\Gamma_2 \leftrightarrow \Gamma_{34}$ have the same hfs in both polarizations (Fig. 3a), but the structure of the lines $\Gamma_{34} \to \Gamma_{34}$ in the sum of the hfs levels in one polarization and the difference in the other (Fig. 3b). The distances between the hfs components of the line are given by

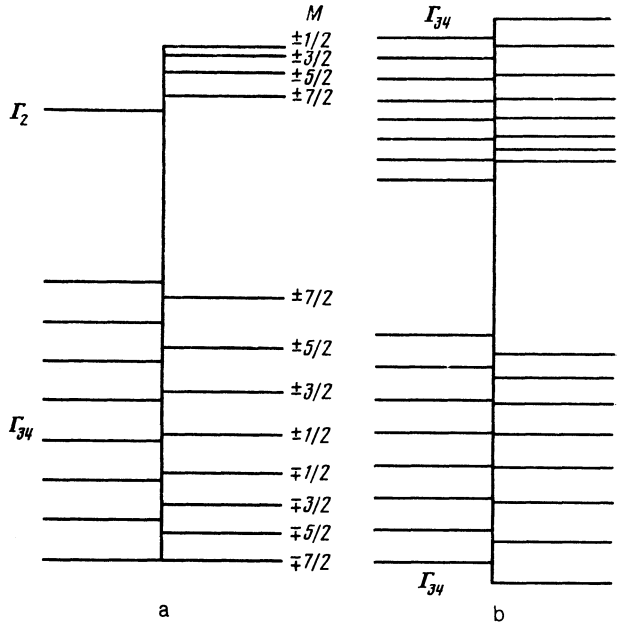

FIG. 2. Hyperfine structure of interacting levels Γ_{34} and Γ_2 of different symmetry (a) and Γ_{34} of like symmetry (b). (The left halves of the figures show the hfs of the unperturbed levels.)

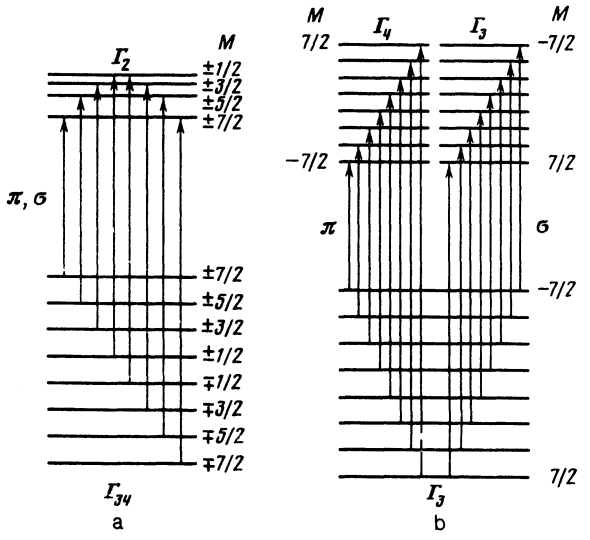

FIG. 3. Level scheme illustrating the formation of hfs lines: (a) $\Gamma_{34} \leftrightarrow \Gamma_2(\Gamma_1)$; (5152.3, 5163.3, 8670.9, 8687.7 cm^{-1} etc.); (b) $\Gamma_{34} \leftrightarrow \Gamma_{34}$ (5155.7, 5184.6 cm^{-1}).

TABLE I. Parameters of hfs of the lines in $LiYF_4:Ho^{3+}$.

	Experiment					Theory							
	Γ	E, cm^{-1}	$E-E_0$, cm^{-1}	a, cm^{-1}	$k\cdot10^3$, cm^{-1}	$E-E_0$, cm^{-1}	A, cm^{-1}	$B\cdot10^3$, cm^{-1}	$C\cdot10^3$, cm^{-1}	$D\cdot10^3$, cm^{-1}	a, cm^{-1}	$k\cdot10^3$, cm^{-1}	$\varphi''\cdot10^{-18}$, V·cm^{-2}
$^5I_6$	2	8796.6	81.9	–	–	80.7	–	–	–	–	–	–	–
	34	8783.7	69.0	–	–	68.9	−0.020	–	–	–	–	–	–
	1	8769.0	54.3	–	–	54.2	0	–	–	–	–	–	–
	2	8702.0	−12.6	0.147	0.8	−18.8	0	1.40	2.01	0.18	–	1.5	2.1
	1	8697.4	−17.3	0.146	−1.7	−13.5	0	0.27	0.48	0.47	–	−1.7	0.4
	2	8687.7	−26.9	0.147	−1.7	−26.1	0	2.06	−1.40	0.70	–	−2.3	3.1
	$34^{(2)}$	8685.9	−28.8	–	–	−30.0	0.118	0.69	1.50	−0.90	0.033	1.5	1.0
	$34^{(1)}$	8680.3	−34.4	0.130	−5.3	−35.9	0.004	−0.25	−1.52	1.45	0.145	−4.8	0.4
	$2\rightarrow34^{(2)}$	8679.0	–	0.094	5.0	–	–	–	–	–	0.117	5.4	–
	1	8673.3	−41.4	0.148	0	−37.7	0	−0.11	−0.55	−1.18	0.150	0.1	0.2
	2	8670.9	−43.8	0.146	−1.3	−44.8	0	−0.13	−0.63	−0.75	0.150	−0.8	0.2
$^5I_7$	1	5293.1	78.3	–	–	78.7	–	–	–	–	–	–	–
	34	5292.9	78.1	–	–	77.8	–	–	–	–	–	–	–
	2	5291.0	76.2	–	–	74.5	–	–	–	–	–	–	–
	2	5232.6	17.8	–	–	17.8	–	–	–	–	–	–	–
	34	5227.8	13.0	–	–	11.7	−0.106	–	–	–	0.256	–	–
	1	5206.1	−8.7	–	–	−9.3	0	–	–	–	0.150	–	–
	$34^{(2)}$	5184.7	−30.1	0.284	0	−29.9	−0.101	1.02	0.32	−0.02	0.251	−0.2	1.5
	$2\rightarrow34^{(2)}$	5177.8	–	0.132	3.2	–	–	–	–	–	0.101	3.7	–
	2	5163.3	−51.5	0.143	1.2	−51.2	0	1.05	1.92	−0.02	0.150	1.4	1.6
	1	5162.8	−51.9	0.150	−4.0	−52.0	0	−0.39	−0.25	1.16	0.150	−4.5	0.6
	$34^{(1)}$	5155.7	−59.0	0.235	−2.1	−59.5	0.076	0.08	−0.36	0.41	0.226	−2.2	0.1
	2	5152.3	−62.5	0.148	0.4	−64.6	0	0.51	−2.03	−1.82	0.150	0.6	0.8
	$2\rightarrow34^{(1)}$	5148.9	–	0.087	1.9	–	–	–	–	–	0.076	1.7	–
$^5I_8$	2	6.8	–	–		–	0	0.05	−1.01	0.70	–	–	0.1
	34	0		0.148±0.003 [12]		–	−0.149	0.57	0	−0.98	–	–	0.9

$$\Delta(M,\ M-1)=a+2k(M-{}^1/_2), \qquad (13)$$

where $k=k_2-k_1$, $a=a_2\pm a_1$ (the plus and minus signs are for the electrodipole and magnetodipole transitions, respectively), while a_2, k_2 and a_1, k_1 are the factors preceeding M and M^2 in Eq. (11) or (12) for the energy of the final and initial levels of the transition.

Our measured distances between the hyperfine components of the different lines in the $^5I_8\rightarrow{}^5I_{7,6}$ transitions are well described by Eq. (13) with constant coefficients. These coefficients, determined from the experimental data, are listed in Table I. Their accuracy is governed by the point scatter due to the spectral noise, and amounts to ±0.001 (±0.003) cm^{-1} in the multiplet $^5I_6$ ($^5I_7$) for the coefficient a and $\pm0.5\cdot10^{-3}$ ($\pm0.8\cdot10^{-3}$) cm^{-1} for k. For transitions from the ground level (Γ_{34}, Ref. 12) we indicate only the symmetry of the final level, and for the transitions of the next energy level, Γ_2 (Ref. 12), separated 6.8 cm^{-1} from the ground level, we indicate the symmetries of the initial and final levels. The additional index in the parentheses numbers repeating representations when an ambiguity is possible. E_0 is the center of gravity of the multiplet.

We have also calculated the hfs of the levels with allowance for quadrupole interaction and off-diagonal matrix elements of the magnetic hyperfine interaction. The wave functions needed for the calculation were obtained from the crystal-field theory, and for the $^5I_7$ level account was taken of J-J mixing with the levels $^5I_6$ and $^5I_7$ that are closest in energy. A successive-approximation procedure was used: The initial set of crystal-field parameters B_n^m (Ref. 9) was first used to calculate the corrections to the Stark-sublevel energies for J-J mixing. The necessary matrix elements were calculated with the aid of computer-programmed $3j$ and $6j$ symbols and tables.[13] No account was taken here of the deviation, which is small for the ^5I term, from he L-S coupling.[14] The corrections obtained (which reached several cm^{-1}) were subtracted from the experimental energies, and the coefficients B_n^m were varied until best agreement was obtained between the resultant energies and the eigenvalues of the crystal-field matrix. The corrections calculated for J-J mixing with the new set of coefficients B_n^m ($B_2^0=172$, $B_4^0=-69$, $B_6^0=-1.5$, $B_4^4=-963$, $B_6^4=-447+109i$), differed little from the initial ones. Allowance for the J-J mixing improved substantially the agreement between the calculated and experimental levels of

TABLE II. Calculated values of certain constants for Ho^{3+} in hfs theory.

	$^5I_8$	$^5I_7$	$^5I_6$
$\langle J\|\|N\|\|J\rangle$	0.767	0.819	0.917
$\langle J\|\|\Lambda\|\|J\rangle$ [14]	1.242	1.175	1.073
$\langle J\|\|\Lambda\|\|J\rangle_{L-S}$	1.250	1.179	1.071
$\langle J\|\|\alpha\|\|J\rangle$ [14, 17]	$-2.04\cdot10^{-3}$	$-2.46\cdot10^{-3}$	$-3.23\cdot10^{-3}$
A_s', cm^{-1}	$-0.83\cdot10^{-3}$	$-0.60\cdot10^{-3}$	$-0.23\cdot10^{-3}$
A_J, cm^{-1}	0.0280 [12]	0.0302	0.0343
B_J, cm^{-1}	0.064	0.059	0.056

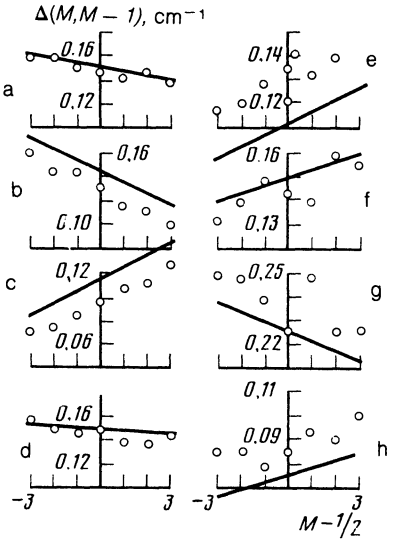

FIG. 4. Distances between neighboring hyperfine components of several lines in $^5I_8 \rightarrow {}^5I_{7,6}$ transitions in an $LiYF_4:Ho^{3+}$ crystal. Points—experiment, lines—hfs calculated with the aid of wave functions obtained from the crystal-field theory for different frequencies (in cm^{-1}): a) 8697.4; b) 8680.3; c) 8679.0; d) 8670.9; e) 5177.8; f) 5163.3; g) 5155.75; h) 5148.9.

the $^5I_7$ multiplet. The $^5I_6$ multiplet was calculated without allowance for the J-J mixing.[9]

The wave functions obtained in this manner were used to calculate, within the limits of one Stark multiplet, the matrix elements contained in expression (4). The sums in the coefficients C and D in (11) and (12) were calculated using the experimental energy values. The constant $A_J(^5I_8)$ is known from ESR data.[12] It was obtained for the levels $^5I_{7,6}$ from Eqs. (2), using the value $g_I = \mu_I/\beta_I I = 1.17$ (Ref. 15). The necessary reduced matrix elements $\langle J\|\Lambda\|J\rangle$ were taken from Ref. 14, where they were calculated with allowance for intermediate coupling. They differ only in their third significant figures from those of $\langle J\|\Lambda\|J\rangle_{L-S}$, calculated by us using the L-S coupling wave functions. The latter functions were used to calculate the reduced matrix elements $\langle J\|N\|J\rangle$. In the calculation of B_J from Eq. (3) we substituted the values $Q = 3.51\cdot10^{-24}$ cm^2 (Ref. 15) and $1 - R_q = 0.95$ (Refs. 15, 16) and the value $\langle r^{-3}\rangle = 6.8\cdot10^{25}$ $cm^{-3} = 9.85\, a_0^{-3}$ obtained from (2). No account was taken of the contribution of the lattice to the electric-field gradient at the nucleus. The calculated constants are listed in Table II.

In Table I above are given the calculated energies of the Stark levels, their magnetic hyperfine splittings A, the quadrupole contributions B to the hfs, and the contributions C and D due to the interactions of levels of like and unlike symmetry. It can be seen that all the parameters that govern the nonequidistance of the hfs are of the same order of magnitude. In the last columns of Table I are given the calculated coefficients a and k of (13), which can be compared with the experimental ones. The agreement between experiment and theory is quite satisfactory. The measured coefficient k, which characterizes the nondequidistance of the hfs, agrees in the overwhelming majority of cases with the calculated one within the limits of experimental error (see also Fig. 4).

The crystal-field theory can thus be successfully used to calculate the hyperfine structure.

Using the expression for the quadrupole correction to the energy of the hyperfine sublevel in terms of the electric-field gradient φ'' at the nucleus (Ref. 18)

$$\Delta E_{qu} = \frac{eQ\varphi''}{2I(2I-1)}\left[M^2 - \frac{I(I+1)}{3}\right], \qquad (14)$$

and comparing it with the quadrupole term in (4), we have estimated the values of φ'' on the basis of the quadrupole corrections calculated in accordance with the crystal-field theory. The good agreement between the experimentally observed nonequidistance of the lines in the hfs and the theoretically calculated one suggests that this estimate is fairly accurate.

In conclusion, the authors thank A. M. Tkachuk for supplying the crystal for the investigation, G. N. Zhenin for interest in the work, and E. P. Ivanova for the program for the calculation of the $3j$ and $6j$ symbols.

[1]A. M. Tkachuk, M. V. Petrov, and A. V. Khil'ko, in: Spectroscopy of Crystals [in Russian], Nauka, 1983, p. 106.
[2]N. Karayianis, D. E. Wortman, and H. P. Jenssen, J. Phys. Chem. Sol. **37**, 7 675 (1976).
[3]H. Caspers and H. Rast, J. Lumin., **10**, 347 (1975).
[4]A. K. Kupchikov, B. Z. Malkin, D. A. Rzaev, and A. I. Ryskun, Fiz. Tverd. Tela (Leningrad), **24**, 2373 (1982) [Sov. Phys. Solid State **24**, 1348 (1982)].
[5]A. P. Abramov, I. N. Abramova, I. Ya. Gerlovin, and I. K. Razumova, Pis'ma Zh. Eksp. Teor. Fiz. **40**, 178 (1984) [JETP Lett. **40**, 937 (1984)].
[6]L. M. Holmes, J. Als-Nielsen, and H. J. Guggenheim, Phys. Rev. **B12**, 180 (1975).
[7]A. H. Cooke, D. A. Jones, J. F. Silva, and M. R. Wells, J. Phys. **C8**, 4083 (1975).
[8]J. Als-Nielsen, L. M. Holmes, F. K. Larsen, and H. J. Guggenheim, Phys. Rev. **B12**, 191 (1975).
[9]N. I. Agladze and M. N. Popova, Sol. St. Comm. **55**, 1097 (1985).
[10]A. A. Balashov, V. S. Bukreev, V. A. Vagin, *et al.*, Prib. Tekh. Eksp. No. 3, 239 (1983).
[11]A. Abragam and B. Bleaney, *Electron Paramagnetic Resonance of Transition Ions*, Oxford, 1970, Vol. 2.
[12]J. Magarino, J. Tuchendler, J. P. D'Haenens, and A. Linz, Phys. Rev. **B13**, 2805 (1976).
[13]C. W. Nielson and G. F. Koster, *Spectroscopic Coefficients for p^n, d^n, f^n Configurations*, MIT Press, 1063.
[14]K. Rajnak and W. F. Krupke, J. Chem. Phys. **46**, 3532 (1967).
[15]B. Burghardt, S. Buttgenbach, N. Glaeser, *et al.* Z. Phys. **A307**, 193 (1982).
[16]J. F. Wyart and P. Camus, Physica **92C**, 227 (1978).
[17]G. H. Dieke, *Spectra and Energy Levels of Rare Earth Ions in Crystals*, Interscience, 1968.
[18]I. I. Sobel'man, Introduction to the theory of Atomic Spectra [in Russian], GIFML, 1963, p. 257 [Engl. Transl., Pergamon, 1973].

Translated by J. G. Adashko